Interference Exploitation MU-MISO Precoding Under Per-Antenna Power Constraint

Yunsi Wen*, Haonan Wang*, Ang Li*, Xuewen Liao*, and Christos Masouros†
School of Information and Communications Engineering, Xi'an Jiaotong University, Xi'an, China*
Department of Electronic and Electrical Engineering, University College London, London, UK†
Email: {yunsiwen, whn8215858}@stu.xjtu.edu.cn*, {ang.li.2020, yeplos}@xjtu.edu.cn*, c.masouros@ucl.ac.uk†

***Abstract*—This paper studies the constructive interference (CI) precoding under per-antenna power constraint (PAPC) in the downlink of multi-user multiple-input single-output (MU-MISO) systems. The scenario of PAPC is more practical than that under sum power constraint (SPC) in actual systems. In this paper, we extend the mathematical precoding structure analysis of CI precoding under SPC to PAPC. By analyzing the formulated optimization problem with KKT conditions and generalized matrix inverse theory, we obtain the closed-form structure of the CI-PAPC precoder as a function of introduced variables and simplify the problem. Then, the primal-dual interior point method (IPM) is employed to solve this simplified problem more efficiently. Simulation results verify our mathematical derivations and show that the proposed method enjoys much lower complexity while maintaining the same communication performance, which promotes the practical implementation of CI precoding in realistic scenarios.**

***Index Terms*—MIMO, constructive interference, per-antenna power constraint, primal-dual IPM, closed-form solutions.**

I. Introduction

With the evolution of wireless communications, the limited spectrum cannot meet the increasing demand for transmission rate. For this reason, MIMO technology has been introduced to improve the spectrum efficiency of communication systems in recent years [1]. However, interference in MIMO is a limiting factor and precoding is required to handle it in multi-user MIMO communications. Dirty paper coding (DPC) can achieve the system capacity theoretically, but it is challenging to implement in practice because of its prohibitive complexity [2]. Unlike non-linear precoding, linear precoding schemes represented by zero-forcing (ZF) and regularized ZF (RZF) make a promising tradeoff between the performance and the complexity such that they are often deployed practically [3].

The studies from DPC reveal that we can achieve the optimal capacity by coding along the direction of interference, which motivates us to rethink the role of interference in wireless systems. The concept of constructive interference was first proposed in [4], where the multiple access interference (MAI) in CDMA systems is divided into constructive interference (CI) and destructive interference (DI). Since the initial idea of CI precoding is to preserve CI while eliminate DI, a modified ZF precoder called selective channel inversion is presented in [5]. Moreover, literature [6] proposes an advanced CI metric for PSK modulations, where the conception of the constructive region is presented, and the 'phase rotation' metric is given. In [7], CI precoding is extended to multi-level modulations, and the 'symbol scaling' metric is introduced. In CI precoding, a convex optimization problem needs to be solved to obtain the optimal precoding matrix, and the update of the precoding matrix is on a symbol level, which results in unfavorable computation complexity. The low-complexity closed-form iterative precoder of CI precoding for phase rotation metric is proposed in [8], where the optimal solution can be obtained in only a few iterations. Literature [9] extends the work of [8] to multi-level modulations. Moreover, [10] proposes a block-level approach to exploit CI where the precoding matrix is constant within a given transmission block. Besides, deep learning-based methods can also be employed to reduce the complexity of CI-based optimization problems [11].

The precoding schemes mentioned above currently consider the sum power constraint (SPC), where the transmit power is enforced on the antenna array in each slot. However, each transmitter antenna is equipped with a dedicated power amplifier in realistic scenarios [12], which means that the per-antenna power constraint (PAPC) scenario is more suitable in practice. Under PAPC, most papers study the precoding design to optimize a specific objective function [13]. Furthermore, in recent years there are also some studies for CI-based precoding with PAPC, which contains per-antenna power minimization under Quality-of-Service constraints [14], the max-min fair problem under PAPC [15], weighted per-antenna power minimization and spatial peak-to-average power ratio minimization [16]. Specifically, [17] proposes computationally efficient CI-PAPC precoding based on the phase-rotation metric for PSK signaling, where the original CI-PAPC problem is transformed by approximating the objective function as a smooth convex function. However, the use of approximations means that the solution obtained in [17] is not optimal, which results in performance loss.

In this paper, we extend the phase rotation metric of CI precoding under SPC to the scenario of PAPC for PSK signaling. First of all, we formulate the CI-PAPC optimization problem under the phase rotation metric. By using the KKT conditions and leveraging a theorem in generalized inverse theory [18], the closed-form structure of the CI-PAPC precoder is obtained as a function of introduced variables, and the original problem is further simplified. Then, the primal-dual interior point method (IPM) [19] is employed to solve the simplified problem, where we design an available initial point selection scheme to speed up the convergence of the primal-dual IPM. Numerical results demonstrate that our method

reduces the complexity while maintaining the identical BER performance compared with the original optimization problem.

II. System Model

Throughout this paper, we consider a downlink MU-MISO system, where the transmitter is equipped with N_t antennas and communicates with K single-antenna users simultaneously in the same time-frequency resource. When CSI is ideally provided at the transmitter, the received signal vector $\mathbf{r} = [r_1, r_2, \cdots, r_K]^T$ can be expressed as

$$\mathbf{r} = \mathbf{HWs} + \mathbf{n}, \tag{1}$$

where $\mathbf{s} = [s_1, s_2, \cdots, s_K]^T$ is the transmitted data symbol vector, and $s_i \in \mathcal{C}^{1\times 1}$ that has been normalized is the symbol for user i. $\mathbf{W} \in \mathcal{C}^{N_t \times K}$ denotes the precoding matrix. $\mathbf{H} = [\mathbf{h}_1, \mathbf{h}_2, \cdots, \mathbf{h}_K]^T$ is the channel matrix where a flat-fading Rayleigh channel is assumed, and each entry in $\mathbf{H} \in \mathcal{C}^{K\times N_t}$ follows the standard complex Gaussian distribution. Additionally, $\mathbf{n} = [n_1, n_2, \cdots, n_K]^T$ denotes additive Gaussian noise vector, and $n_i \in \mathcal{C}^{1\times 1}$ is the noise with zero mean and variance σ^2 at user i.

CI refers to the interference that can push the constellation points at the receiver away from the system detection boundaries. Fig. 1 shows the schematic diagram of the phase rotation metric under PSK modulations. In the case of strict phase rotation, the phase of the received noiseless signal is enforced to be strictly aligned with that of the interested transmitted signal. When the constructive region (the green region in Fig. 1) is introduced to relax the condition of strict phase rotation, the phase of the received noiseless signal is no longer strictly aligned with that of the desired signal, which is the non-strict phase rotation metric. For example, in Fig. 1, the phase of $\vec{OB}$ is strictly aligned with that of $\vec{OS}$, which means the condition of strict phase rotation can be expressed as $\mathbf{h}_k^T\mathbf{Ws} = \lambda_k s_k$ [8], where λ_k is a real number satisfying $\lambda_k \geq t$, and $s_k = \vec{OS}$. On the other hand, while the phase of $\vec{OC}$ is not equal to that of $\vec{OS}$, point C is still confined to the constructive region. Therefore, the corresponding condition of non-strict phase rotation can be similarly given by $\mathbf{h}_k^T\mathbf{Ws} = \lambda_k s_k$ [8], but in this case λ_k becomes a complex number satisfying $\left|\Im(\lambda_k)\right| - (\Re(\lambda_k) - t)\tan\theta_t \leq 0$, where $\left|\Im(\lambda_k)\right| = \left|\vec{CD}\right|$, $\Re(\lambda_k) = \left|\vec{OD}\right|$, $\left|\lambda_k\right| = \left|\vec{OC}\right|$, $\theta_t = \pi/M$, and M is the modulation order for M-PSK modulations.

III. CI-PAPC Precoding for PSK Modulations

In this section, we focus on the design of CI-PAPC precoding under PSK modulations, where the non-strict phase rotation metric is considered. Moreover, since the strict phase rotation is a particular case of the non-strict phase rotation, the corresponding optimization problem can be solved similarly.

A. Optimal Closed-Form Structure for $\mathbf{W}$

With the non-strict phase rotation metric, the optimization problem of CI-PAPC precoding that aims to make the received

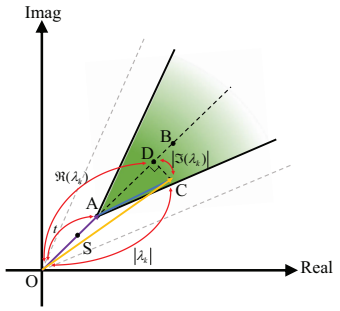

Fig. 1: Schematic diagram of phase rotation metric, 8PSK.

constellation points located in the CI region can be expressed as

$$\begin{aligned}
\mathcal{P}_1: \min_{\mathbf{W},t}\ & -t \\
s.t. & \ \mathbf{h}_k^T\mathbf{Ws} - \lambda_k s_k = 0,\ \forall k \in \mathcal{K} && \text{(2a)}\\
& \left|\lambda_k^{\Im}\right| - \left(\lambda_k^{\Re} - t\right)\tan\theta_t \leq 0,\ \forall k \in \mathcal{K} && \text{(2b)}\\
& \left\|\mathbf{e}_n^T\mathbf{Ws}\right\|_2^2 \leq P,\ \forall n \in \mathcal{N} && \text{(2c)}
\end{aligned}$$

where $P = p_0/N_t$ is the maximum permitted power at each antenna, p_0 represents the maximum available power per symbol slot, $\mathbf{e}_n$ denotes the n-th column of the identity matrix, $\mathcal{K} = \{1, 2, \cdots, K\}$, and $\mathcal{N} = \{1, 2, \cdots, N_t\}$. Then, we decompose the precoding matrix $\mathbf{W}$ into column vectors, which is $\mathbf{W} = [\mathbf{w}_1, \mathbf{w}_2, \cdots, \mathbf{w}_K]$. Based on the virtual multicast formulation presented in [6] and the fact that $\mathbf{Ws} = \sum_{i=1}^K \mathbf{w}_i s_i$, without loss of generality we assume each $\mathbf{w}_i s_i$ is identical such that (2c) can be transformed into

$$\mathbf{e}_n^T\left(\sum_{i=1}^K \mathbf{w}_i s_i \left(\mathbf{w}_i s_i\right)^H\right)\mathbf{e}_n \leq \frac{P}{K}. \tag{3}$$

Furthermore, we construct the Lagrangian function of $\mathcal{P}_1$ as

$$\begin{aligned}
\mathcal{L}\left(\mathbf{w}_i, t, \delta_k, \mu_k, \nu_n\right) = & -t + \sum_{k=1}^K \delta_k\left(\mathbf{h}_k^T\sum_{i=1}^K \mathbf{w}_i s_i - \lambda_k s_k\right) \\
& + \sum_{k=1}^K \mu_k\left(\left|\lambda_k^{\Im}\right| - \left(\lambda_k^{\Re} - t\right)\tan\theta_t\right) \\
& + \sum_{n=1}^{N_t} \nu_n\left(\mathbf{e}_n^T\left(\sum_{i=1}^K \mathbf{w}_i s_i \left(\mathbf{w}_i s_i\right)^H\right)\mathbf{e}_n - \frac{P}{K}\right)
\end{aligned} \tag{4}$$

where δ_k, μ_k and ν_n are the Lagrangian multipliers, and the power constraints (2c) are substituted by (3). With (4), we express partial KKT conditions that we will employ in the following as

$$\frac{\partial\mathcal{L}}{\partial\mathbf{w}_i} = \sum_{k=1}^K \delta_k\mathbf{h}_k s_i + \sum_{n=1}^{N_t} \nu_n s_i s_i^*\left(\mathbf{e}_n\mathbf{e}_n^T\right)\mathbf{w}_i^* = 0,\ \forall i \in \mathcal{K} \tag{5a}$$

$$\mathbf{h}_k^T\sum_{i=1}^K \mathbf{w}_i s_i - \lambda_k s_k = 0,\ \forall k \in \mathcal{K} \tag{5b}$$

$$\nu_n\left(\mathbf{e}_n^T\left(\sum_{i=1}^K \mathbf{w}_i s_i \left(\mathbf{w}_i s_i\right)^H\right)\mathbf{e}_n - \frac{P}{K}\right) = 0,\ \forall n \in \mathcal{N} \tag{5c}$$

By defining a diagonal matrix $\mathbf{D} = \sum_{n=1}^{N_t} \nu_n \cdot \left(\mathbf{e}_n \mathbf{e}_n^T\right) = diag\left(\nu_1, \nu_2, \cdots, \nu_{N_t}\right)$, (5a) can be further transformed into $\mathbf{D}\mathbf{w}_i = -\frac{1}{s_i}\sum_{k=1}^{K} \delta_k^* \mathbf{h}_k^*$, where each ν_n is a real number such that $\mathbf{D} = \mathbf{D}^*$. When optimality of $\mathcal{P}_1$ is achieved, we can observe that the power constraint of each antenna is not always active under PAPC, which means when the complementary slackness conditions (5c) are considered, $\mathbf{D}$ is rank-deficient as partial diagonal elements in $\mathbf{D}$ are zero. Thus, we cannot directly obtain the structure of $\mathbf{w}_i$ by taking the inverse of D.

Proposition 1: There exists a matrix $\mathbf{D}_\mathbf{1}^\star$ such that the optimal $\mathbf{w}_i$ can be formulated as

$$\mathbf{w}_i = \mathbf{D}_\mathbf{1}^\star \cdot \left(-\frac{1}{s_i}\sum_{k=1}^{K} \delta_k^* \mathbf{h}_k^*\right). \tag{6}$$

Proof: Firstly, we can regard $\mathbf{D}\mathbf{w}_i = -\frac{1}{s_i}\sum_{k=1}^{K} \delta_k^* \mathbf{h}_k^*$ as a set of linear equations to vector $\mathbf{w}_i$, which has infinite solutions as $\mathbf{D}$ is rank-deficient. Then, according to the definition of generalized inverse matrix [18], there exists a generalized inverse of $\mathbf{D}$ satisfying $\mathbf{D}\mathbf{D_1}\mathbf{D} = \mathbf{D}$ such that all the solutions of $\mathbf{w}_i$ can be expressed as $\mathbf{w}_i = \mathbf{D_1} \cdot \left(-\frac{1}{s_i}\sum_{k=1}^{K} \delta_k^* \mathbf{h}_k^*\right)$, where the number of such feasible $\mathbf{D_1}$ is also infinite. Therefore, there must be a generalized inverse matrix $\mathbf{D}_\mathbf{1}^\star$ corresponding to the optimal $\mathbf{w}_i$, which completes the proof. ■

Although proposition 1 proves the existence of $\mathbf{D}_\mathbf{1}^\star$, finding an exact expression for that is unnecessary because $\mathbf{D}_\mathbf{1}^\star$ will be substituted as will be shown in the following. Based on (6), we can derive $\mathbf{w}_i s_i = \mathbf{D}_\mathbf{1}^\star \cdot \left(\sum_{k=1}^{K} \delta_k^* \mathbf{h}_k^*\right)$, and due to our assumption that each $\mathbf{w}_i s_i$ is identical, we can obtain that (6) holds for each $\mathbf{w}_i$. Then, by introducing $\mathbf{\Theta} = -\sum_{k=1}^{K} \delta_k^* \mathbf{D}_\mathbf{1}^\star \mathbf{h}_k^*$ and $\hat{\mathbf{s}} = \left[\frac{1}{s_1}, \frac{1}{s_2}, \cdots, \frac{1}{s_K}\right]$, the precoding matrix is given by

$$\begin{aligned}\mathbf{W} &= [\mathbf{w}_1, \mathbf{w}_2, \cdots, \mathbf{w}_K] \\ &= -\sum_{k=1}^{K} \delta_k^* \mathbf{D}_\mathbf{1}^\star \mathbf{h}_k^* \cdot \left[\frac{1}{s_1}, \frac{1}{s_2}, \cdots, \frac{1}{s_K}\right] \\ &= \mathbf{\Theta}\hat{\mathbf{s}}. \end{aligned} \tag{7}$$

To proceed, we express (5b) in a compact form, which is

$$\mathbf{H}\mathbf{W}\mathbf{s} = diag(\mathbf{\Lambda})\mathbf{s}, \tag{8}$$

where $\mathbf{\Lambda} = [\lambda_1, \lambda_2, \cdots, \lambda_K]^T$. By substituting (7) into (8) and considering $\hat{\mathbf{s}}\mathbf{s} = K$, we can further obtain

$$\mathbf{H}\mathbf{\Theta} = \frac{1}{K} diag(\mathbf{\Lambda})\mathbf{s}. \tag{9}$$

Consequently, when the scenario of $N_t = K$ is considered, we can directly obtain the precoding matrix as

$$\mathbf{W} = \mathbf{\Theta}\hat{\mathbf{s}} = \frac{1}{K}\mathbf{H}^{-1} diag(\mathbf{\Lambda})\mathbf{s}\hat{\mathbf{s}}. \tag{10}$$

However, since the dimension of $\mathbf{H}$ is $K \times N_t$, it is challenging to get the structure of $\mathbf{\Theta}$ under $N_t > K$ as (9) to $\mathbf{\Theta}$ has infinite solutions.

Proposition 2: For the scenario of $N_t \geq K$, the optimal structure of the CI-PAPC precoding matrix under PSK modulations can be formulated as

$$\mathbf{W} = \left[\frac{1}{K}\mathbf{H}^H \left(\mathbf{H}\mathbf{H}^H\right)^{-1} diag(\mathbf{\Lambda})\mathbf{s} + \mathbf{M} \cdot \mathbf{y}\right]\hat{\mathbf{s}}, \tag{11}$$

where $\mathbf{M} = \mathbf{I} - \mathbf{H}^H \left(\mathbf{H}\mathbf{H}^H\right)^{-1}\mathbf{H}$, and $\mathbf{y} \in \mathcal{C}^{N_t \times 1}$ is a newly introduced optimization variable.

Proof: First of all, we consider the case of $N_t > K$. If the system of linear equations $\mathbf{A}\mathbf{x} = \mathbf{b}$ has solutions, the general solutions of this system can be expressed as $\mathbf{x} = \mathbf{A_1}\mathbf{b} + (\mathbf{I} - \mathbf{A_1}\mathbf{A})\mathbf{y}$, where $\mathbf{A_1}$ is the generalized inverse of $\mathbf{A}$ satisfying $\mathbf{A}\mathbf{A_1}\mathbf{b} = \mathbf{b}$ [18]. With (9), we can similarly obtain the corresponding general solution to $\mathbf{\Theta}$ as

$$\mathbf{\Theta} = \frac{1}{K}\mathbf{H_1} diag(\mathbf{\Lambda})\mathbf{s} + (\mathbf{I} - \mathbf{H_1}\mathbf{H})\mathbf{y}, \tag{12}$$

where for convenience, we set the generalized inverse $\mathbf{H_1} = \mathbf{H}^H \left(\mathbf{H}\mathbf{H}^H\right)^{-1}$. Thus, we can directly obtain the precoding structure as (11). For the case of $N_t = K$, the precoding matrix (11) can be transformed into (10) due to $\mathbf{M} = \mathbf{0}$, and then we complete the proof. ■

To proceed with (11), firstly, we can obtain that

$$\begin{aligned}\mathbf{W}\mathbf{s} &= \mathbf{H}^H \left(\mathbf{H}\mathbf{H}^H\right)^{-1} diag(\mathbf{\Lambda})\mathbf{s} + K\mathbf{M}\mathbf{y} \\ &= \mathbf{H}^H \left(\mathbf{H}\mathbf{H}^H\right)^{-1} diag(\mathbf{s})\mathbf{\Lambda} + K\mathbf{M}\mathbf{y} \\ &= \mathbf{\Phi}\mathbf{u}, \end{aligned} \tag{13}$$

where $\mathbf{\Phi} = \left[\mathbf{H}^H \left(\mathbf{H}\mathbf{H}^H\right)^{-1} diag(\mathbf{s}) \quad K\mathbf{M}\right]$ and $\mathbf{u} = \left[\mathbf{\Lambda}^T, \mathbf{y}^T\right]^T$. Then, the power constraints (2c) can be further transformed into $\mathbf{u}^H\mathbf{Q}_n\mathbf{u} \leq P$, where $\mathbf{Q}_n = \mathbf{\Phi}^H \mathbf{e}_n \mathbf{e}_n^T \mathbf{\Phi}$, and $\mathbf{u}$ is a complex vector such that we need to turn $\mathbf{u}^H\mathbf{Q}_n\mathbf{u} \leq P$ into real-valued constraints. Therefore, letting

$$\hat{\mathbf{u}} = \begin{bmatrix}\Re(\mathbf{u}) \\ \Im(\mathbf{u})\end{bmatrix}, \quad \hat{\mathbf{Q}}_n = \begin{bmatrix}\Re(\mathbf{Q}_n) & -\Im(\mathbf{Q}_n) \\ \Im(\mathbf{Q}_n) & \Re(\mathbf{Q}_n)\end{bmatrix}, \tag{14}$$

we can obtain $\hat{\mathbf{u}}^T\hat{\mathbf{Q}}_n\hat{\mathbf{u}} \leq P$ that is equivalent to $\mathbf{u}^H\mathbf{Q}_n\mathbf{u} \leq P$, and then $\mathcal{P}_1$ can be simplified as

$$\begin{aligned}\mathcal{P}_2 : &\min_{\hat{\mathbf{u}}, t} -t \\ &s.t. \left|\lambda_k^\Im\right| - \left(\lambda_k^\Re - t\right)\tan\theta_t \leq 0, \ \forall k \in \mathcal{K} \qquad (15a) \\ &\hat{\mathbf{u}}^T\hat{\mathbf{Q}}_n\hat{\mathbf{u}} \leq P, \ \forall n \in \mathcal{N} \qquad (15b)\end{aligned}$$

However, since the dual of $\mathcal{P}_2$ is not quadratic programming, it is challenging to follow the derivation in [8]. Consequently, in this paper, we resort to the primal-dual interior point method to solve $\mathcal{P}_2$. To begin with, based on the fact that $\hat{\mathbf{u}} = \left[\Re(\mathbf{\Lambda}^T) \quad \Re(\mathbf{y}^T) \quad \Im(\mathbf{\Lambda}^T) \quad \Im(\mathbf{y}^T)\right]^T$, by introducing $\hat{\mathbf{E}}_\mathbf{1} = \left[\mathbf{I}_K \quad \mathbf{0} \quad \mathbf{0} \quad \mathbf{0}\right]$ and $\hat{\mathbf{E}}_\mathbf{2} = \left[\mathbf{0} \quad \mathbf{0} \quad \mathbf{I}_K \quad \mathbf{0}\right]$, we can obtain $\Re(\mathbf{\Lambda}) = \hat{\mathbf{E}}_\mathbf{1}\hat{\mathbf{u}}$ and $\Im(\mathbf{\Lambda}) = \hat{\mathbf{E}}_\mathbf{2}\hat{\mathbf{u}}$ such that (15a) can be further transformed into

$$\hat{\mathbf{E}} \cdot \hat{\mathbf{u}} + t \cdot \mathbf{1} \leq \mathbf{0}, \tag{16}$$

where we define $\hat{\mathbf{E}} = -\begin{bmatrix}-\hat{\mathbf{E}}_\mathbf{2}/\tan(\theta_t) - \hat{\mathbf{E}}_\mathbf{1} \\ \hat{\mathbf{E}}_\mathbf{2}/\tan(\theta_t) - \hat{\mathbf{E}}_\mathbf{1}\end{bmatrix}$. Furthermore, by introducing $\mathbf{a} = \begin{bmatrix}0 & \cdots & 0 & -1\end{bmatrix}^T$, $\hat{\mathbf{T}} = \begin{bmatrix}-\hat{\mathbf{E}} & \mathbf{1}\end{bmatrix}$, $\hat{\mathbf{x}} =$

$\left[\hat{\mathbf{u}}^T \quad t\right]^T$, $\hat{\mathbf{Z}}_n = \begin{bmatrix} \hat{\mathbf{Q}}_n & \mathbf{0} \\ \mathbf{0} & 0 \end{bmatrix}$, we can rewrite $\mathcal{P}_2$ as

$$\mathcal{P}_3 : \min_{\hat{\mathbf{x}}} \mathbf{a}^T \hat{\mathbf{x}}$$
$$s.t.\ \mathbf{g}(\hat{\mathbf{x}}) = \begin{bmatrix} \hat{\mathbf{x}}^T \hat{\mathbf{Z}}_1 \hat{\mathbf{x}} - P \\ \vdots \\ \hat{\mathbf{x}}^T \hat{\mathbf{Z}}_{N_t} \hat{\mathbf{x}} - P \\ \hat{\mathbf{T}} \hat{\mathbf{x}} \end{bmatrix} \preceq \mathbf{0} \tag{17}$$

B. Primal-Dual IPM for Solving $\mathcal{P}_3$

In this paper, we consider the basic primal-dual IPM proposed in [19]. Based on $\mathcal{P}_3$, we first construct the Lagrangian function as

$$\mathcal{L} = \mathbf{a}^T \hat{\mathbf{x}} + \mathbf{\Psi}^T \mathbf{g}(\hat{\mathbf{x}}), \tag{18}$$

where $\mathbf{\Psi} = [\psi_1, \psi_2, \cdots, \psi_{N_t+2K}]^T$. Therefore, the modified KKT conditions can be formulated as

$$\begin{bmatrix} \mathbf{r}_{dual} \\ \mathbf{r}_{cent} \end{bmatrix} = \begin{bmatrix} \mathbf{a} + \mathbf{J}^T(\hat{\mathbf{x}}) \mathbf{\Psi} \\ -diag(\mathbf{\Psi}) \mathbf{g}(\hat{\mathbf{x}}) - (1/t_p) \cdot \mathbf{1} \end{bmatrix} = \begin{bmatrix} \mathbf{0} \\ \mathbf{0} \end{bmatrix}, \tag{19}$$

where $\mathbf{r}_{dual}$ and $\mathbf{r}_{cent}$ are the dual residual and centrality residual, respectively. t_p is a positive parameter related to the duality measure, and $\mathbf{J}(\hat{\mathbf{x}})$ is the Jacobian matrix of $\mathbf{g}(\hat{\mathbf{x}})$. By taking the first order Taylor series expansion of (19), we can obtain that

$$\begin{bmatrix} \sum_{i=1}^{N_t} 2\psi_i \hat{\mathbf{Z}}_i & \mathbf{J}^T(\hat{\mathbf{x}}) \\ -diag(\mathbf{\Psi}) \mathbf{J}(\hat{\mathbf{x}}) & -diag(\mathbf{g}(\hat{\mathbf{x}})) \end{bmatrix} \begin{bmatrix} \triangle \hat{\mathbf{x}} \\ \triangle \mathbf{\Psi} \end{bmatrix} = - \begin{bmatrix} \mathbf{r}_{dual} \\ \mathbf{r}_{cent} \end{bmatrix}. \tag{20}$$

Furthermore, by combining (19) and (20), we can derive the Newton search direction as follows:

$$\mathbf{R} \cdot \triangle \hat{\mathbf{x}} = -\mathbf{a} + \frac{1}{t_p} \mathbf{J}^T(\hat{\mathbf{x}}) \mathbf{G} \tag{21}$$

$$\triangle \mathbf{\Psi} = -\mathbf{\Psi} - \frac{1}{t_p} \mathbf{G} - diag(\mathbf{g}(\hat{\mathbf{x}}))^{-1} diag(\mathbf{\Psi}) \mathbf{J}(\hat{\mathbf{x}}) \cdot \triangle \hat{\mathbf{x}} \tag{22}$$

where

$$\mathbf{R} = \sum_{i=1}^{N_t} 2\psi_i \hat{\mathbf{Z}}_i - \mathbf{J}^T(\hat{\mathbf{x}}) diag(\mathbf{g}(\hat{\mathbf{x}}))^{-1} diag(\mathbf{\Psi}) \mathbf{J}(\hat{\mathbf{x}}) \tag{23}$$

and $\mathbf{G} = diag(\mathbf{g}(\hat{\mathbf{x}}))^{-1} \mathbf{1}$. However, we find $\mathbf{R}$ is rank-deficient in practice, which leads to the fact that $\triangle \hat{\mathbf{x}}$ cannot be directly obtained by multiplying $\mathbf{R}^{-1}$ by the right side of (21). Consequently, the pseudo-inverse of $\mathbf{R}$ is adopted to obtain $\triangle \hat{\mathbf{x}}$, that is

$$\triangle \hat{\mathbf{x}} = \mathbf{R}^{\dagger} \cdot (-\mathbf{a} + \frac{1}{t_p} \mathbf{J}^T(\hat{\mathbf{x}}) \mathbf{G}). \tag{24}$$

We summarize the basic primal-dual IPM in Algorithm 1. For $\mathcal{P}_3$, the selection of the initial point must guarantee $\mathbf{g}(\hat{\mathbf{x}}) \prec \mathbf{0}$, i.e., $\hat{\mathbf{x}}^T \hat{\mathbf{Z}}_n \hat{\mathbf{x}} - P < 0, n \in \mathcal{N}$ and $\hat{\mathbf{T}} \hat{\mathbf{x}} \prec \mathbf{0}$. Firstly, the constraints $\hat{\mathbf{x}}^T \hat{\mathbf{Z}}_n \hat{\mathbf{x}} - P < 0, n \in \mathcal{N}$ are equivalent to $\hat{\mathbf{u}}^T \hat{\mathbf{Q}}_n \hat{\mathbf{u}} < P, n \in \mathcal{N}$, where we set $\hat{\mathbf{u}} = a \cdot \mathbf{1}$ for convenience, and then the power constraints can be expressed as

$$\begin{aligned} &\hat{\mathbf{u}}^T \hat{\mathbf{Q}}_n \hat{\mathbf{u}} < P, \quad n \in \mathcal{N} \\ &\Rightarrow a < \sqrt{\frac{P}{\mathbf{1}^T \hat{\mathbf{Q}}_n \mathbf{1}}}, \quad n \in \mathcal{N} \\ &\Rightarrow a < \sqrt{\frac{P}{\max_{n \in \mathcal{N}} \{\mathbf{1}^T \hat{\mathbf{Q}}_n \mathbf{1}\}}}. \end{aligned} \tag{25}$$

We define $a_0 = \sqrt{\frac{P}{\max_{n \in \mathcal{N}} \{\mathbf{1}^T \hat{\mathbf{Q}}_n \mathbf{1}\}}}$ and multiply a_0 by a scaling parameter γ satisfying $\gamma < 1$ such that the initial $\hat{\mathbf{u}}$ is given by $\hat{\mathbf{u}}_{\mathbf{0}} = a_0 \gamma \cdot \mathbf{1}$. On the other hand, the constraints $\hat{\mathbf{T}} \hat{\mathbf{x}} \prec \mathbf{0}$ are equivalent to $\left|\lambda_k^{\Im}\right| - \left(\lambda_k^{\Re} - t\right) \tan\theta_t < 0, k \in \mathcal{K}$, where with $\hat{\mathbf{u}}_{\mathbf{0}} = a_0 \gamma \cdot \mathbf{1}$ the initial t_0 must be a negative number. Combining $\hat{\mathbf{u}}_{\mathbf{0}} = a_0 \gamma \cdot \mathbf{1}$ and $t_0 < 0$, we can finally obtain the initial point as $\hat{\mathbf{x}}_{\mathbf{0}} = [\hat{\mathbf{u}}_{\mathbf{0}}^T, t_0]^T$. As for $\mathbf{\Psi}_{\mathbf{0}}$, we set $[\mathbf{\Psi}_{\mathbf{0}}]_i = -1/[\mathbf{g}(\hat{\mathbf{x}}_{\mathbf{0}})]_i, i = 1, \cdots, N_t + 2K$. Moreover, the backtracking line search is adopted to determine the step length s, where $\alpha \in [0.01, 0.1]$, $\beta \in [0.3, 0.8]$ [19].

Algorithm 1 Primal-Dual Interior Point Method

Input: $\mathbf{s}$, $\mathbf{H}$
Output: $\hat{\mathbf{x}}$
1: Choose a strictly feasible initial point $\hat{\mathbf{x}}_{\mathbf{0}}$ and $\mathbf{\Psi}_{\mathbf{0}}$;
2: Initialize $i = 0$, $m = size(\mathbf{g}(\hat{\mathbf{x}}), 1)$, μ, ε;
3: **while** $\max\{\|\mathbf{r}_{dual}\|_2, \|\mathbf{r}_{cent}\|_2\} > \varepsilon$ and $i < i_{max}$ **do**
4: $i \leftarrow i + 1$;
5: Compute $t_p = \mu m / \eta$, $\eta = -\mathbf{g}(\hat{\mathbf{x}})^T \cdot \mathbf{\Psi}$;
6: Compute $\triangle \hat{\mathbf{x}}$ and $\triangle \mathbf{\Psi}$ based on (22) and (24);
7: Determine step length s (backtracking line search);
8: Update $\hat{\mathbf{x}} \leftarrow \hat{\mathbf{x}} + s \cdot \triangle \hat{\mathbf{x}}$, $\mathbf{\Psi} \leftarrow \mathbf{\Psi} + s \cdot \triangle \mathbf{\Psi}$;
9: **end while**

IV. Numerical Results

In this section, based on Monte Carlo simulations, the numerical results of our proposed method are presented to evaluate the practical performance. In each symbol slot, we assume $p_0 = 1$, and then the transmit SNR can be expressed as $\rho = 1/\sigma^2$. The corresponding parameters in primal-dual IPM iterations are $\alpha = 0.05$, $\beta = 0.75$, $\gamma = 0.1$, $\mu = 5$, $t_0 = -1$, $\varepsilon = 10^{-6}$, and $i_{max} = 60$. We obtain all the simulation results from the PC with an i7-12700K CPU and 32GB RAM.

For convenience, we employ the following abbreviations in our simulation results:

1) 'ZF-PAPC': ZF precoder satisfying the PAPC, that is

$$\mathbf{W}_{\mathrm{ZF-PAPC}} = \sqrt{p_0/N_t} \cdot \beta_{\mathrm{ZF-PAPC}} \cdot \mathbf{H}^{\dagger}, \tag{26}$$

where $\beta_{\mathrm{ZF-PAPC}} = 1/(\max_{i \in \mathcal{N}} \left|\left[\mathbf{H}^{\dagger}\mathbf{s}\right]_i\right|)$ is a positive scaling parameter [20].

2) 'RZF-PAPC': RZF precoder satisfying the PAPC, that is

$$\mathbf{W}_{\mathrm{RZF-PAPC}} = \sqrt{p_0/N_t} \cdot \beta_{\mathrm{RZF-PAPC}} \cdot \mathbf{W}_{\mathrm{RZF}}, \tag{27}$$

where we denote that $\mathbf{W}_{\mathrm{RZF}} = \mathbf{H}^H(\mathbf{H}\mathbf{H}^H + \frac{K}{\rho} \cdot \mathbf{I})^{-1}$ and $\beta_{\mathrm{RZF-PAPC}} = 1/(\max_{i \in \mathcal{N}} |[\mathbf{W}_{\mathrm{RZF}}\mathbf{s}]_i|)$.

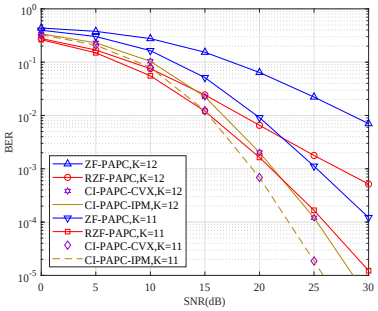

Fig. 2: BER v.s. SNR, $N_t = 12$, QPSK.

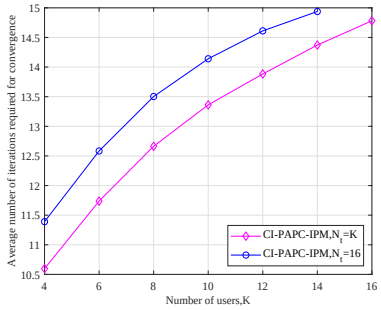

Fig. 3: Average number of iterations, QPSK.

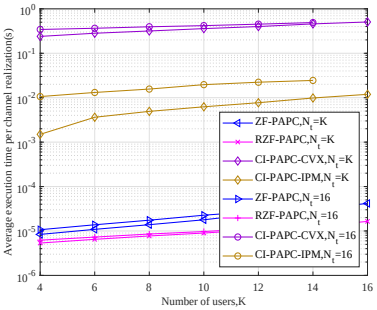

Fig. 4: Average execution time, QPSK.

3) 'CI-PAPC-CVX(or IPM)': constructive interference precoding with per-antenna power constraint solved by CVX (or our proposed primal-dual IPM), where the non-strict phase notation metric is employed.

Fig. 2 shows the BER of the ZF-PAPC precoder, RZF-PAPC precoder and CI-PAPC precoder under QPSK. When SNR $>$ 15 dB, the CI-PAPC precoder can achieve a better performance than the other precoders. Moreover, for the scenarios of $N_t = K$ and $N_t > K$, the primal-dual IPM achieves the identical performance as CVX, which verifies the availability of our proposed scheme.

Fig. 3 shows the average number of iterations in the primal-dual IPM. Overall, the primal-dual IPM requires only a dozen iterations to obtain the optimal solution within our antenna configurations. Moreover, since the dimension of the optimization variable has increased under $N_t > K$ due to the introduction of vector $\mathbf{y}$, the scenario of $N_t > K$ needs more iterations compared with that of $N_t = K$.

Fig. 4 shows the average execution time of the above precoders. In comparison with CVX, our proposed method reduces the average execution time by one or two orders of magnitude. Furthermore, for $N_t > K$, the performance gain of the primal-dual IPM over CVX is decreased compared to $N_t = K$ as the dimension of the problem has increased.

V. Conclusion

This paper investigates the CI precoding under PAPC scenario. By analyzing the KKT conditions, we derive the structure of the optimal precoding matrix and simplify the original problem. Then, the primal-dual IPM is employed to solve this simplified problem. In the simulation results, our proposed scheme reduces the complexity while maintaining the same BER performance compared with the original problem, which promotes the implementation of CI-PAPC precoding in practical systems.

References

[1] L. Zheng and D. N. C. Tse, "Diversity and Multiplexing: A Fundamental Tradeoff in Multiple-Antenna Channels," *IEEE Transactions on Information Theory*, vol. 49, no. 5, pp. 1073–1096, May 2003.

[2] M. Costa, "Writing on dirty paper," *IEEE Transactions on Information Theory*, vol. 29, no. 3, pp. 439–441, May 1983.

[3] C. Peel, B. Hochwald, and A. Swindlehurst, "A vector-perturbation technique for near-capacity multiantenna multiuser communication-part i: channel inversion and regularization," *IEEE Transactions on Communications*, vol. 53, no. 1, pp. 195–202, Jan. 2005.

[4] C. Masouros and E. Alsusa, "A novel transmitter-based selective-precoding technique for ds/cdma systems," *IEEE Signal Processing Letters*, vol. 14, no. 9, pp. 637–640, Sep. 2007.

[5] C. Masouros and E. Alsusa, "Dynamic linear precoding for the exploitation of known interference in mimo broadcast systems," *IEEE Transactions on Wireless Communications*, vol. 8, no. 3, pp. 1396–1404, Mar. 2009.

[6] C. Masouros and G. Zheng, "Exploiting known interference as green signal power for downlink beamforming optimization," *IEEE Transactions on Signal Processing*, vol. 63, no. 14, pp. 3628–3640, July 2015.

[7] M. Alodeh, S. Chatzinotas, and B. Ottersten, "Symbol-level multiuser miso precoding for multi-level adaptive modulation," *IEEE Transactions on Wireless Communications*, vol. 16, no. 8, pp. 5511–5524, Aug. 2017.

[8] A. Li and C. Masouros, "Interference exploitation precoding made practical: Optimal closed-form solutions for psk modulations," *IEEE Transactions on Wireless Communications*, vol. 17, no. 11, pp. 7661–7676, Nov. 2018.

[9] A. Li, C. Masouros, B. Vucetic, Y. Li, and A. L. Swindlehurst, "Interference exploitation precoding for multi-level modulations: Closed-form solutions," *IEEE Transactions on Communications*, vol. 69, no. 1, pp. 291–308, Jan. 2021.

[10] A. Li, C. Shen, X. Liao, C. Masouros, and A. Lee Swindlehurst, "Practical interference exploitation precoding without symbol-by-symbol optimization: A block-level approach," *IEEE Transactions on Wireless Communications*, 2022.

[11] Z. Bo, R. Liu, M. Li, and Q. Liu, "Deep learning based efficient symbol-level precoding design for mu-miso systems," *IEEE Transactions on Vehicular Technology*, vol. 70, no. 8, pp. 8309–8313, Aug. 2021.

[12] B. Li, H. H. Dam, K. L. Teo, and A. Cantoni, "A survey on zero-forcing beamformer design under per-antenna power constraints for multiuser mimo systems," in *2015 IEEE International Conference on Digital Signal Processing (DSP)*, July 2015, pp. 329–333.

[13] W. Yu and T. Lan, "Transmitter optimization for the multi-antenna downlink with per-antenna power constraints," *IEEE Transactions on Signal Processing*, vol. 55, no. 6, pp. 2646–2660, June 2007.

[14] D. Spano, M. Alodeh, S. Chatzinotas, and B. Ottersten, "Per-antenna power minimization in symbol-level precoding," in *2016 IEEE Global Communications Conference (GLOBECOM)*, Dec. 2016, pp. 1–6.

[15] D. Spano, S. Chatzinotas, J. Krause, and B. Ottersten, "Symbol-level precoding with per-antenna power constraints for the multi-beam satellite downlink," in *2016 8th Advanced Satellite Multimedia Systems Conference and the 14th Signal Processing for Space Communications Workshop (ASMS/SPSC)*, Sep. 2016, pp. 1–8.

[16] D. Spano, M. Alodeh, S. Chatzinotas, and B. Ottersten, "Symbol-level precoding for the nonlinear multiuser miso downlink channel," *IEEE Transactions on Signal Processing*, vol. 66, no. 5, pp. 1331–1345, Mar. 2018.

[17] C.-E. Chen, "Computationally efficient constructive interference precoding for psk modulations under per-antenna power constraint," *IEEE Transactions on Vehicular Technology*, vol. 69, no. 8, pp. 9206–9211, Aug. 2020.

[18] A. Ben-Israel and T. N. E. Greville, *Generalized inverses : Theory and Applications*, 2nd ed. USA: Springer, 2003.

[19] S. Boyd and L. Vandenberghe, *Convex Optimization*. U.K.: Cambridge Univ. Press, 2004.

[20] S.-R. Lee, J.-S. Kim, S.-H. Moon, H.-B. Kong, and I. Lee, "Zero-forcing beamforming in multiuser miso downlink systems under per-antenna power constraint and equal-rate metric," *IEEE Transactions on Wireless Communications*, vol. 12, no. 1, pp. 228–236, Jan. 2013.